

Critical domain-wall dynamics of model B

R. H. Dong, B. Zheng,* and N. J. Zhou

Zhejiang Institute of Modern Physics, Zhejiang University, Hangzhou 310027, People's Republic of China

(Received 16 February 2009; published 22 May 2009)

With Monte Carlo methods, we simulate the critical domain-wall dynamics of model B, taking the two-dimensional Ising model as an example. In the macroscopic short-time regime, a dynamic scaling form is revealed. Due to the existence of the quasirandom walkers, the magnetization shows intrinsic dependence on the lattice size L . An exponent which governs the L dependence of the magnetization is measured to be $\sigma = 0.243(8)$.

DOI: [10.1103/PhysRevE.79.051125](https://doi.org/10.1103/PhysRevE.79.051125)

PACS number(s): 64.60.Ht

According to Hohenberg and Halperin [1], a dynamic system with no conservation laws is called model A, while that with a conserved order parameter is model B. For *critical* systems, the equilibrium state of model B is in the same universality class of model A. For lattice models, such as the Ising model, the critical temperature of model B is also the same as that of model A. However, the dynamic universality class of model B is different from that of model A. For the two-dimensional (2D) ϕ^4 theory, one has derived that the dynamic exponent $z=4-\eta$, with η being the well known static exponent [1]. In other words, z is *not* an independent one, and its value is around 4, much larger than $z \approx 2$ of model A.

The dynamic scaling behavior of model A has been understood around and even *far from* equilibrium [1–5]. Based on the dynamic scaling form in the *macroscopic* short-time regime, new methods for the determination of both dynamic and static critical exponents have been developed [4,6,7]. Recent progress in the short-time critical dynamics includes, for example, theoretical calculations and numerical simulations of the XY models and Josephson junction arrays [8–11], magnets with quenched disorder [12–14], aging phenomena [15–17], and various applications and developments [18–22]. Very recently, critical relaxation of a domain wall has been concerned [23,24], and it is also relevant for the domain-wall dynamics at zero or low temperatures [25,26].

The dynamics of model B is important in various fields. For example, the phase ordering dynamics of model B describes the spinodal decomposition of binary alloys and phase separation of fluids [27,28]. The dynamics of driven lattice gases also belongs to model B [21,29–31]. However, the critical dynamics of model B is less studied in the literature compared to that of model A [15]. This is mainly because its critical slowing down is more severe, and it is difficult to reach the equilibrium. From this view, it is instructive to explore the short-time critical dynamics of model B for the critical slowing down does not disturb so much the simulations [4,6,7]. In Ref. [29], the short-time dynamic scaling form is applied to numerically identify the universality classes of anisotropic driven lattice gases. Since the dynamic system is rather complicated, it induces a controversy [32,33].

Our thought is to clarify the short-time dynamic scaling form of model B starting from simpler systems. For the 2D Ising model, critical relaxation with a *disordered* initial state has been simulated with the Kawasaki algorithm [34–37]. The results support that the dynamic exponent is $z=4-\eta=15/4$. To fully understand the short-time critical dynamics of model B, we should explore the dynamic effects of different initial conditions. An ordered state cannot be the initial state of model B. But the dynamic relaxation with a *semior-dered* initial state is important. In fact, it describes the dynamic evolution of a domain wall. In the case of model A, there emerge plenty of new phenomena [23–26,38].

The purpose of this paper is to investigate the critical domain-wall dynamics of model B with Monte Carlo methods. To be specific, we simulate the dynamic relaxation of the 2D Ising model starting from a semior-dered state with the Kawasaki algorithm. The semior-dered initial state consists of two fully ordered domains with opposite spin orientations. As time evolves, the domain wall between two domains roughens and looks like a growing interface, i.e., the so-called *domain interface*. Such a dynamic process is inhomogeneous in space, very different from that with a disordered initial state.

In Monte Carlo simulations, the 2D Ising model is defined on a rectangular lattice, with a linear size $2L_x$ in the x direction and L_y in the y direction. *Antiperiodic* and periodic boundary conditions are adopted in the x and y directions, respectively. Initially, spins are taken to be positive on the sublattice $L_x \times L_y$ at the right side and negative at the left side. With the semior-dered initial state, we update the spin configuration by exchanging two spins in the nearest neighbor with the heat-bath algorithm at the critical temperature T_c up to a maximum time $t_M=10^6$. Most simulations are performed with $L_x=L_y=L$. The totals of samples for average are 30 000, 20 000, 3000, and 2000 for $L=32, 64, 128, \text{ and } 256$, respectively. Statistical errors are estimated by dividing the samples into two or three subgroups. If the fluctuation in the time direction is comparable with or larger than the statistical error, it will be taken into account. For convenience, we set the x axis such that the domain wall between the positive and negative spins is located at $x=0$. So the x coordinate of a lattice site is a half-integer.

For simplicity, we first set $L_x=L_y=L$. Due to the semior-dered initial state, the time evolution of the dynamic system is inhomogeneous in the x direction. Therefore we measure the magnetization as a function of x and t ,

*Corresponding author; zheng@zimp.zju.edu.cn

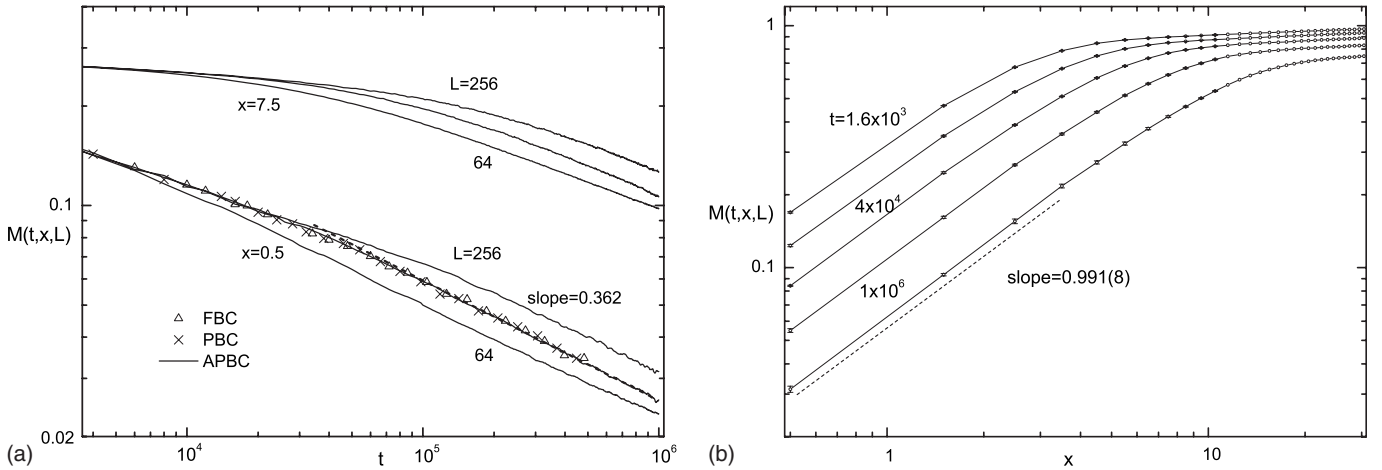


FIG. 1. (a) The time evolution of the magnetization is plotted for different x , and $L=64$, 128, and 256 (from below) on a double-logarithmic scale. An antiperiodic boundary condition (APBC) is adopted in the x direction. For comparison, results of $x=0.5$ and $L=128$ with periodic and free boundary conditions (PBC and FBC) are also included. The dashed line shows a power-law fit. (b) The magnetization obtained with $L=256$ is plotted versus x for different t on a double-logarithmic scale. Errors of the data points are less or about 1%. The dashed line shows a power-law fit.

$$M(t,x,L) = \frac{1}{L} \left\langle \left[\sum_{y=1}^L S_{xy}(t) \right] \right\rangle. \quad (1)$$

Here $S_{xy}(t)$ is the spin at the time t on the lattice site (x,y) and $\langle \dots \rangle$ represents the statistical average. Generally, the magnetization may depend on L .

At the critical temperature, there are three spatial scales in the dynamic system, i.e., the nonequilibrium correlation length $\xi(t)$, the coordinate x , and the lattice size L . One may believe that $\xi(t)$ grows in a universal form $\xi(t) \sim t^{1/z}$ in all spatial directions because of the homogeneity of the interactions in the Hamiltonian. Therefore, standard scaling arguments lead to the scaling form of the magnetization,

$$M(t,x,L) = t^{-\beta/\nu z} \tilde{M}(t^{1/z}/x, t^{1/z}/L), \quad (2)$$

where β and ν are the static exponents and z is the dynamic exponent. For the 2D Ising model with the dynamics of model B, theoretical values of the exponents are $\beta=1/8$, $\nu=1$, and $z=15/4$. On the right side of the above equation, the overall factors $t^{-\beta/\nu z}$ indicates the scaling dimension of M and the scaling function $\tilde{M}(s,u)$ describes the scale invariance of the dynamic system. In the macroscopic long-time regime, i.e., the regime with $\xi(t) \geq L$, it has been well known that the dynamic system exhibits a universal dynamic scaling behavior. In this paper, we assume that the scaling form in Eq. (2) holds already in the macroscopic short-time regime, i.e., the regime with $\xi(t) \ll L$, after a microscopic time scale t_{mic} .

For the dynamics of model A, the dynamic scaling behavior of the magnetization is relatively simple. In the short-time regime, the finite-size effect of $M(t,x,L)$ is negligible because of $\xi(t) \ll L$. $M(t,x,L) \rightarrow t^{-\beta/\nu z} F(s)$ with $s=t^{1/z}/x$. For a large s , i.e., inside the domain interface, $F(s)$ exhibits a power-law behavior $F(s) \sim s^{-\beta_0/\nu}$, with $\beta_0/\nu \approx 1$. For a small s , i.e., outside the domain interface, $F(s) \sim \text{const}$ [23]. In the

long-time regime, the magnetization may depend on the lattice size L , typically dominated by an exponential law $M(t,L) \sim \exp(-t/L^z)$. For the dynamics of model B, the dynamic scaling behavior of the magnetization is rather complicated. It is anomalous that the magnetization shows intrinsic dependence on the lattice size L even in the short-time regime. In Fig. 1(a), the time evolution of the magnetization is displayed. For a fixed x , $M(t,x,L)$ obviously varies with L . Although $M(t,x,L)$ strongly depends on L , it is insensitive to the boundary condition. In Fig. 1(a), numerical simulations with periodic and free boundary conditions in the x direction are also included. All boundary conditions lead to the same results.

The domain-wall motion of model B is driven by interchanging positive and negative spins in neighbor. When a negative spin escapes from the domain interface and jumps into the positive domain, it becomes *quasifree* and moves *randomly*. We call this spin a *quasirandom walker*. The average moving distance of the quasirandom walkers in a time t is the order of $l_r(t) \sim \sqrt{t}$. Even in the short-time regime, i.e., the regime with $\xi(t) \sim t^{1/z} \ll L$, it may occur $L < l_r(t) \sim \sqrt{t}$ for the dynamic exponent $z=15/4 > 2$. Therefore the quasirandom walkers easily touch the boundary of the dynamic system. This should be the physical origin of the L dependence of the magnetization in the short-time regime.

In fact, the average moving distance $l_r(t)$ of the quasirandom walkers is an additional spatial scale for the dynamics of model B. In the literatures, such a diffusion length scale $l_r(t) \sim t^{\phi/z}$ with $\phi \approx z/2$ has been detected in the dynamic relaxation with a disordered initial state [15,37]. In principle, the magnetization should also depend on the scaling variable $l_r(t)/L$. The dynamic scaling form in Eq. (2) holds only when the quasirandom walkers reach a ‘‘homogeneous’’ state, i.e., $l_r(t) \gg L$. In other words, the quasirandom walkers should touch the boundary, turn back to the domain interface, and then stabilize at a homogenous state. At $x=0.5$, for example, the shortest time t_S for this movement is about $t_S=4L^2$ in our numerical simulations.

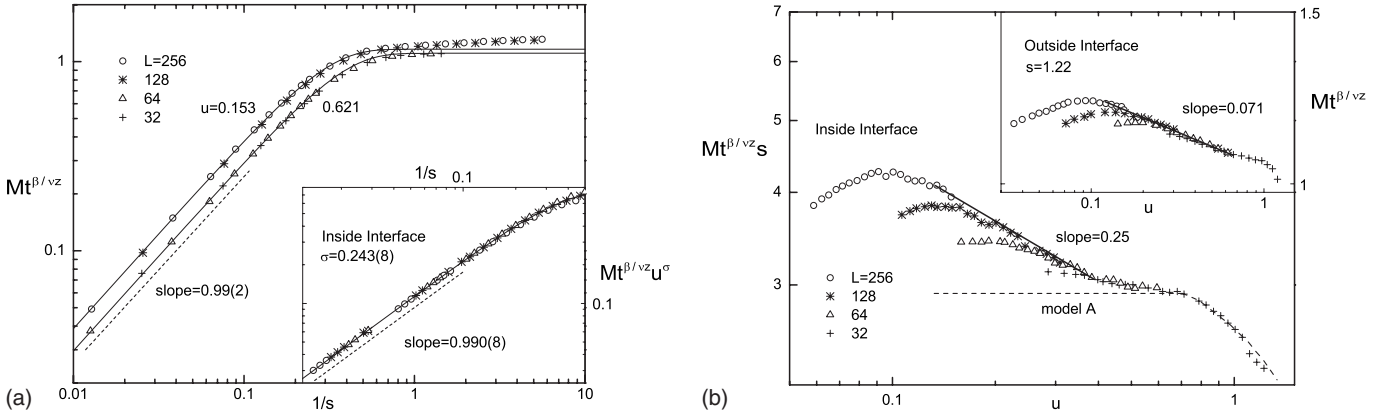


FIG. 2. (a) The scaling function $M(t, x, L)t^{\beta/\nu z} = \tilde{M}(s, u)$ with $s = t^{1/z}/x$ and $u = t^{1/z}/L$ is plotted versus $1/s$ for fixed $u = 0.53$ and 0.621 . Data collapse is observed for different L . Solid lines represent the error function $f(y) \sim \int^y \exp(-x^2) dx$ and the dashed line shows a power-law fit. In the inset, a power-law behavior $\tilde{M}(s, u) \sim F(s)u^{-\sigma}$ is assumed in the short-time regime, and data of different u and L inside the domain interface collapse onto a single curve $Mt^{\beta/\nu z}u^\sigma \sim F(s)$. (b) A power-law behavior $\tilde{M}(s, u) \sim G(u)s^{-1}$ is assumed inside the domain interface, and data of different L collapse onto the master curve $Mt^{\beta/\nu z}s \sim G(u)$. The solid line indicates the power-law behavior in the short-time regime. Departure of the data from the master curve in the time regime $t < t_S \sim 4L^2$ is also displayed. The dashed line schematically shows the scaling function of model A. In the inset, the scaling function $\tilde{M}(s, u)$ outside the domain interface is plotted versus u .

Since $M(t, x, L)$ relies on t through two scaling variables in Eq. (2), its dynamic behavior is complicated. Nevertheless, a dynamic scaling form is typically characterized by power-law behaviors. Let us now concentrate on the following features of the scaling function $\tilde{M}(s, u)$,

$$\tilde{M}(s, u) \rightarrow \begin{cases} G(u)s^{-\beta_0/\nu} & s \rightarrow \infty \\ F(s)u^{-\sigma} & s \rightarrow \infty, u \rightarrow 0 \end{cases} \quad (3)$$

with $s = t^{1/z}/x$ and $u = t^{1/z}/L$. Actually, $F(s) = s^{-\beta_0/\nu}$. We use the notation $F(s)$ for convenience. The exponent β_0/ν characterizes the spatial behavior of the magnetization inside the domain interface, which appears similar to the surface exponent defined on a surface [20, 23, 24]. Thus we call it the interface exponent. σ is an exponent exclusive for the dynamics of model B for describing the finite-size dependence of the magnetization.

In Fig. 1(b), the magnetization is plotted versus x . Inside the domain interface, i.e., for $x \ll \xi(t)$ or a large s , $M(t, x, L)$ exhibits a power-law behavior. The slope of the curves is $0.991(8)$, very close to 1. This suggests $\beta_0/\nu = 1$ and indicates that $M(t, x, L)$ is an analytic function of x , the same as that of model A [23]. In Fig. 1(a), we detect a power-law decay of the magnetization inside the domain interface in the short-time regime, i.e., for large s and small u . The slope is estimated to be 0.362 from the curve of $L = 128$. For $L = 64$, it is reaching the long-time regime for $t > 10^5$, and a deviation from the power law is observed. This power-law behavior indicates $(\beta/\nu + \beta_0/\nu + \sigma)/z \approx 0.362$ and yields $\sigma \approx 0.242$ with the input $\beta/\nu = 1/8$ and $z = 15/4$. Since σ is positive, the magnetization in Eq. (3) increases with L . Therefore we call this L dependence of the magnetization *intrinsic*.

To illustrate the scaling form comprehensively and precisely, we now perform scaling plots with Eq. (2). In Fig. 2(a), the scaling function $\tilde{M}(s, u)$ with a fixed u is displayed, and data collapse is observed for different L . In the large- s

regime, i.e., inside the domain interface, $\tilde{M}(s, u)$ exhibits a power-law behavior $s^{-\beta_0/\nu}$ with $\beta_0/\nu = 0.99(2)$. This agrees with the measurement in Fig. 1(b). For the dynamics of model A, the scaling function $\tilde{M}(s)$ can be fitted to the error function [23, 24]. For the dynamics of model B, $\tilde{M}(s, u)$ with a fixed u also coincides with the error function in the large- s regime. However, it does not approach a constant in the small- s regime due to the existence of the quasirandom walkers.

According to Eq. (3), $\tilde{M}(s, u) \sim F(s)u^{-\sigma}$ for large s and small u . In the inset of Fig. 2(a), the scaling plot for $M(t, x, u)t^{\beta/\nu z}u^\sigma \sim F(s)$ is performed. Data collapse is observed inside the domain interface. With the input $\beta/\nu = 1/8$ and $z = 15/4$, we extract the exponents $\sigma = 0.243(8)$ and $\beta_0/\nu = 0.990(8)$, consistent with 0.242 and $0.991(8)$ estimated from Figs. 1(a) and 1(b).

To explicitly reveal the L dependence of the magnetization in different time regimes, we fix s and plot the scaling function $\tilde{M}(s, u)$ versus u . Inside the domain interface, i.e., for a large s , $\tilde{M}(s, u) \sim G(u)s^{-1}$. In Fig. 2(b), the scaling function $M(t, x, u)t^{\beta/\nu z}s \sim G(u)$ is displayed at $x = 0.5$. In the time regime $t > t_S \sim 4L^2$, data collapse is observed. For a small u , there emerges a power-law decay $G(u) \sim u^{-\sigma}$, and σ is estimated to 0.25 , in agreement with $0.243(8)$ extracted from Fig. 2(a). For a large u , $G(u)$ is governed by an exponential law. For comparison, a scaling function $G(u)$ of model A is schematically shown in Fig. 2(b). In the time regime $t < t_S$, the scaling form is violated due to the quasirandom walkers, and data of different L do not collapse. To fully understand the dynamic behavior in this time regime, we need to include the additional scaling variable $l_r(t)/L$ in the dynamic scaling form. A detailed description of this kind will be presented elsewhere.

In the inset of Fig. 2(b), the scaling function of model B is plotted for a small s , i.e., outside the domain interface. Quali-

tatively, $G(u)$ is similar to that inside the domain interface, but the effective σ decreases with s .

Finally, we should point out that the finite-size dependence of the magnetization in the domain-wall motion of model B is anisotropic in spatial directions. In fact, the intrinsic L dependence of the scaling function $\tilde{M}(s, u)$ in Eq. (3) does refer only to L_x , not L_y . Since the domain wall is oriented in the y direction, the random walkers does not induce anomalous dependence of the magnetization on L_y . In the short-time regime, i.e., the regime with $\xi(t) \ll L_y$, the magnetization is *independent of L_y* . In Monte Carlo simulations, we have confirmed this by fixing L_x and changing L_y from 64 to 128 and 256.

In summary, we have simulated the critical domain-wall dynamics of model B with Monte Carlo methods, taking the

2D Ising model as an example. A short-time dynamic scaling form is revealed, and the scaling function is carefully computed. Due to the existence of the quasirandom walkers, the magnetization intrinsically depends on the lattice size even in the short-time regime. This is very different from the case of model A. The exponent σ which governs the L dependence of the magnetization is measured to be 0.243(8). The interface exponent β_0/ν takes the value 0.99(1), close to 1, the same as that of model A. It is a challenge to derive the scaling form in Eq. (2) and extract the exponent σ in Eq. (3) with renormalization group methods.

This work was supported in part by NNSFC under Grant Nos. 10875102 and 10325520.

-
- [1] P. C. Hohenberg and B. I. Halperin, *Rev. Mod. Phys.* **49**, 435 (1977).
- [2] H. K. Janssen, B. Schaub, and B. Schmittmann, *Z. Phys. B: Condens. Matter* **73**, 539 (1989).
- [3] D. A. Huse, *Phys. Rev. B* **40**, 304 (1989).
- [4] B. Zheng, *Int. J. Mod. Phys. B* **12**, 1419 (1998).
- [5] B. Zheng, M. Schulz, and S. Trimper, *Phys. Rev. Lett.* **82**, 1891 (1999).
- [6] Z. B. Li, L. Schülke, and B. Zheng, *Phys. Rev. Lett.* **74**, 3396 (1995).
- [7] H. J. Luo, L. Schülke, and B. Zheng, *Phys. Rev. Lett.* **81**, 180 (1998).
- [8] B. Zheng, F. Ren, and H. Ren, *Phys. Rev. E* **68**, 046120 (2003).
- [9] Y. Ozeki and N. Ito, *Phys. Rev. B* **68**, 054414 (2003).
- [10] E. Granato and D. Dominguez, *Phys. Rev. B* **71**, 094521 (2005).
- [11] H. Liu, J. P. Lv, and Q. H. Chen, *EPL* **84**, 66004 (2008).
- [12] J. Q. Yin, B. Zheng, and S. Trimper, *Phys. Rev. E* **72**, 036122 (2005).
- [13] Y. Ozeki and K. Ogawa, *Phys. Rev. B* **71**, 220407(R) (2005).
- [14] Y. Chen and Z. B. Li, *Phys. Rev. B* **71**, 174433 (2005).
- [15] P. Calabrese and A. Gambassi, *J. Phys. A* **38**, R133 (2005).
- [16] X. W. Lei and B. Zheng, *Phys. Rev. E* **75**, 040104(R) (2007).
- [17] F. Roma and D. Dominguez, *Phys. Rev. B* **78**, 184431 (2008).
- [18] H. K. Lee and Y. Okabe, *Phys. Rev. E* **71**, 015102(R) (2005).
- [19] S. L. Fan and F. Zhong, *Phys. Rev. E* **76**, 041141 (2007).
- [20] S. Z. Lin and B. Zheng, *Phys. Rev. E* **78**, 011127 (2008).
- [21] G. Baglietto and E. V. Albano, *Phys. Rev. E* **78**, 021125 (2008).
- [22] E. Arashiro, J. R. Drugowich de Felicio, and U. H. E. Hansmann, *J. Chem. Phys.* **126**, 045107 (2007).
- [23] N. J. Zhou and B. Zheng, *Phys. Rev. E* **77**, 051104 (2008).
- [24] Y. Y. He, B. Zheng, and N. J. Zhou, *Phys. Rev. E* **79**, 021107 (2009).
- [25] T. Nattermann, V. Pokrovsky, and V. M. Vinokur, *Phys. Rev. Lett.* **87**, 197005 (2001).
- [26] W. Kleemann, *Annu. Rev. Mater. Res.* **37**, 415 (2007).
- [27] A. Bray, *Adv. Phys.* **43**, 357 (1994), and references therein.
- [28] A. J. Bray, *Adv. Phys.* **51**, 481 (2002).
- [29] E. V. Albano and G. Saracco, *Phys. Rev. Lett.* **88**, 145701 (2002).
- [30] S. Caracciolo, A. Gambassi, M. Gubinelli, and A. Pelissetto, *Phys. Rev. E* **72**, 056111 (2005).
- [31] T. H. R. Smith, O. Vasilyev, D. B. Abraham, A. Maciolek, and M. Schmidt, *Phys. Rev. Lett.* **101**, 067203 (2008).
- [32] S. Caracciolo, A. Gambassi, M. Gubinelli, and A. Pelissetto, *Phys. Rev. Lett.* **92**, 029601 (2004).
- [33] E. V. Albano and G. Saracco, *Phys. Rev. Lett.* **92**, 029602 (2004).
- [34] F. J. Alexander, D. A. Huse, and S. A. Janowsky, *Phys. Rev. B* **50**, 663 (1994).
- [35] S. N. Majumdar, D. A. Huse, and B. D. Lubachevsky, *Phys. Rev. Lett.* **73**, 182 (1994).
- [36] C. Godrèche, F. Krzakala, and F. Ricci-Tersenghi, *J. Stat. Mech.: Theory Exp.* (2004) P04007.
- [37] C. Sire, *Phys. Rev. Lett.* **93**, 130602 (2004).
- [38] N. J. Zhou, B. Zheng, and Y. Y. He, *EPL* **78**, 56001 (2007).